Published in final edited form as:
Sci Transl Med. 2021 May 19; 13(594): . doi:10.1126/scitranslmed.aaw1564.

Gene therapy restores dopamine transporter expression and ameliorates pathology in iPSC and mouse models of infantile parkinsonism

Joanne Ng[1,2,†], **Serena Barral**[2,*,†], **Carmen De La Fuente Barrigon**[3], **Gabriele Lignani**[4], **Fatma A. Erdem**[2,5], **Rebecca Wallings**[6], **Riccardo Privolizzi**[1,2], **Giada Rossignoli**[2], **Haya Alrashidi**[3], **Sonja Heasman**[2], **Esther Meyer**[2], **Adeline Ngoh**[2], **Simon Pope**[7], **Rajvinder Karda**[1], **Dany Perocheau**[1], **Julien Baruteau**[1], **Natalie Suff**[1,8], **Juan Antinao Diaz**[1], **Stephanie Schorge**[4,9], **Jane Vowles**[10], **Lucy R. Marshall**[11], **Sally A. Cowley**[10], **Sonja Sucic**[5], **Michael Freissmuth**[5], **John R. Counsell**[12], **Richard Wade-Martins**[6], **Simon J.R. Heales**[3,7], **Ahad A. Rahim**[9], **Maximilien Bencze**[12,13], **Simon N. Waddington**[1,14,*,‡], **Manju A. Kurian**[2,15,‡]

[1]Gene Transfer Technology Group, EGA-Institute for Women's Health, University College London, London, WC1E 6HX, UK

[2]Developmental Neurosciences, Zayed Centre for Research into Rare Disease in Children, GOS-Institute of Child Health, University College London, London, WC1N 1DZ, UK

[3]Genetics and Genomic Medicine, GOS-Institute of Child Health, University College London, London, WC1N 1EH, UK

[4]Clinical and Experimental Epilepsy, Queen Square Institute of Neurology, University College London, London, WC1N 3BG, UK

[5]Institute of Pharmacology and Gaston H. Glock Laboratories for Exploratory Drug Research, Centre of Physiology and Pharmacology, Medical University of Vienna, 1090 Vienna, Austria

[6]Oxford Parkinson's Disease Centre, Department of Physiology, Anatomy and Genetics, University of Oxford, Oxford, OX1 3PT, UK

[*]Corresponding author. s.waddington@ucl.ac.uk (S.N.W.); s.barral@ucl.ac.uk (S.B.).
[†]These authors contributed equally to this work.
[‡]These authors contributed equally to this work.

Author contributions: M.A.K. conceived and designed the study. S.N.W. designed the study. J.N. designed and performed experiments and data analysis for the in vivo study. S.B. designed and performed experiments and data analysis for the in vitro study. C.D.L.F.B. and H.A. performed HPLC analysis, supervised by S.P. and S.J.R.H. G.L., and S. Schorge performed patch clamp electrophysiology and analysis. F.A.E., G.R., and S.H. contributed to in vitro experiments. R.W. performed tritiated dopamine uptake analysis, supervised by R.W.-M. J.N., J.R.C., R.P., R.K., D.P., J.B., N.S., J.A.D., A.A.R., and S.N.W. contributed to gene therapy construct design, vector production, in vivo experiments, and analysis. E.M. and A.N. performed Sanger sequencing and data analysis. J.N., S.N.W., S.B., and M.B. performed the teratoma test. J.V. and S.A.C. contributed to iPSC generation. L.R.M. performed cytometric bead assay. S. Sucic and M.F. provided pifithrin-μ. M.B. designed and performed the cytotoxicity assay and undertook data analysis. J.N., S.B., S.N.W., and M.A.K. drafted the manuscript, and F.A.E., R.W., C.D.L.F.B., G.L., A.N., and M.B. contributed to written sections of the manuscript. S. Schorge, S.A.C., M.F., S.J.R.H., R.W.-M., and M.B., provided input for manuscript revision. All authors reviewed the manuscript before submission.

Competing interests: J.N., J.R.C., M.A.K., and S.N.W. are co-inventors on patent application titled "Gene therapy for DTDS (GB2101958.3). M.A.K. was sponsored by Agilis to attend the AADC Deficiency International Advisory Board (AADC-D IAB) on 27 June 2018. S.N.W. has previous or existing consultancy agreements with ONO Pharmaceuticals, Synpromics Ltd., Reliance Biosciences, Codiak Biosciences, Takeda Pharmaceutical Company, and LivaNova Plc. M.A.K. and S.N.W. hold consultancy agreements with Biormarin, and S.N.W. and J.N. also have consultancy agreements with Albion Capital. Sponsored research agreements with Synpromics/Askbio Europe (S.N.W. and J.N.) and Rocket Pharma (R.K., J.N., S.S., and S.N.W.).

Europe PMC Funders Author Manuscripts

[7]Neurometabolic Unit, National Hospital for Neurology and Neurosurgery, Queen Square, London, WC1N 3BG, UK

[8]Department of Women and Children's Health, King's College London, London, WC2R 2LS, UK

[9]Pharmacology, School of Pharmacy, University College London, London, WC1N 1AX, UK

[10]James Martin Stem Cell Facility, Sir William Dunn School of Pathology, University of Oxford, Oxford, OX1 3RE, UK

[11]Infection, Immunity, Inflammation, GOS-Institute of Child Health, University College London, London, WC1N 1EH, UK

[12]Developmental Neurosciences, GOS-Institute of Child Health, University College London, London, WC1N 1EH, UK

[13]University Paris Est Creteil, INSERM, IMRB, 94000 Creteil, France

[14]Wits/SAMRC Antiviral Gene Therapy Research Unit, Faculty of Health Sciences, University of the Witwatersrand, 2193 Johannesburg, South Africa

[15]Department of Neurology, Great Ormond Street Hospital for Children, London, WC1N 3JH, UK

Abstract

Most inherited neurodegenerative disorders are incurable, and often only palliative treatment is available. Precision medicine has great potential to address this unmet clinical need. We explored this paradigm in dopamine transporter deficiency syndrome (DTDS), caused by biallelic loss-of-function mutations in *SLC6A3*, encoding the dopamine transporter (DAT). Patients present with early infantile hyperkinesia, severe progressive childhood parkinsonism, and raised cerebrospinal fluid dopamine metabolites. The absence of effective treatments and relentless disease course frequently leads to death in childhood. Using patient-derived induced pluripotent stem cells (iPSCs), we generated a midbrain dopaminergic (mDA) neuron model of DTDS that exhibited marked impairment of DAT activity, apoptotic neurodegeneration associated with TNFα-mediated inflammation, and dopamine toxicity. Partial restoration of DAT activity by the pharmacochaperone pifithrin-μ was mutation-specific. In contrast, lentiviral gene transfer of wild-type human *SLC6A3* complementary DNA restored DAT activity and prevented neurodegeneration in all patient-derived mDA lines. To progress toward clinical translation, we used the knockout mouse model of DTDS that recapitulates human disease, exhibiting parkinsonism features, including tremor, bradykinesia, and premature death. Neonatal intracerebroventricular injection of human *SLC6A3* using an adeno-associated virus (AAV) vector provided neuronal expression of human DAT, which ameliorated motor phenotype, life span, and neuronal survival in the substantia nigra and striatum, although off-target neurotoxic effects were seen at higher dosage. These were avoided with stereotactic delivery of AAV2.SLC6A3 gene therapy targeted to the midbrain of adult knockout mice, which rescued both motor phenotype and neurodegeneration, suggesting that targeted AAV gene therapy might be effective for patients with DTDS.

Europe PMC Funders Author Manuscripts

Introduction

Most neurodegenerative disorders lack effective disease-modifying treatments. This leads to substantial morbidity, increased risk of mortality, and considerable socioeconomic burden. With deeper understanding of the underlying pathogenic processes, targeted precision medicine strategies are increasingly becoming a clinical reality (1, 2).

Dopamine transporter (DAT) is highly expressed in presynaptic midbrain dopaminergic (mDA) neurons, where it reuptakes released dopamine (DA) from the synaptic cleft. It is a key regulator of the amplitude and duration of dopaminergic transmission (6). To date, 29 cases of dopamine transporter deficiency syndrome (DTDS) have been published (3–5, 7–13) and a further 17 are unpublished, referred to our center between 2015 and 2020. As many reported patients have been misdiagnosed with cerebral palsy (4), the true incidence is likely to be higher. DTDS presents as a progressive movement disorder characterized initially by infantile-onset hyperkinesia, with features of dystonia, choreoathetosis, ballismus, orolingual dyskinesia, and recurrent oculogyric crises. Life-threatening status dystonicus is commonly reported. Severe parkinsonism with akinesia, rigidity, tremor, and hypomimia develops in late childhood or early adolescence. Analysis of neurotransmitter concentrations in cerebrospinal fluid (CSF) characteristically reveals a raised concentration of the DA metabolite, homovanillic acid (HVA), but a normal concentration of serotonin metabolite 5-hydroxyindoleacetic acid (5-HIAA), leading to a pathologically increased CSF HVA:HIAA ratio. The relentless disease course and lack of effective treatments frequently leads to premature death in the first or second decade of life, usually secondary to respiratory complications.

Very little is known about the cellular progression of DTDS in the central nervous system. Progressive changes were measured by single-photon emission computed tomography imaging with ioflupane (I123) (DaTscan) over an 8-year interval in a patient with atypical DTDS (7). Although this is suggestive of progressive nigrostriatal neurodegeneration, postmortem data from patients with DTDS have not yet been available to confirm this clinical observation. To date, our limited understanding of cellular mechanisms underpinning DTDS pathogenesis has hindered the development of effective diseasemodifying or curative therapies.

Here, we have used a patient-derived induced pluripotent stem cell (iPSC) mDA neuronal system in tandem with a murine model of disease to investigate clinically translatable precision medicine strategies for patients with DTDS.

Results

Loss of DAT function and dysregulated DA metabolism is evident in mDA neurons derived from patients with DTDS

Using a patient-derived mDA model, we first explored the effect of mutant DAT protein on neuronal function, comparing patient lines to age-matched and CRISPR-corrected controls.

iPSC lines were generated from dermal fibroblasts of patient with DTDS with homozygous missense mutations in *SLC6A3* (patient 1: c.1103T>A, p.L368Q; patient 2: c.1184C>T, p.P395L) (3). Control iPSCs were similarly generated from an age-matched healthy individual. An isogenic control line was created by CRISPR-Cas9 correction of the c.1184C>T variant in patient 2. Genomic DNA sequencing confirmed that all patient-derived iPSC lines maintained their specific homozygous *SLC6A3* mutation, with successful correction of the mutation in the isogenic control (fig. S1A). All iPSC lines exhibited pluripotency and maintenance of genomic integrity (fig. S1, B to H).

Given the specific expression profile of DAT (6), patient-derived iPSC lines were then differentiated into mDA neurons (14, 15). After 11 days of differentiation, comparable high numbers of mDA progenitors were present in both DTDS patient and control lines (fig. S2, A and B) with typical midbrain precursor gene expression profiles (fig. S2C). After 65 days of differentiation, mature mDA neurons showed a typical gene and protein expression profile, characteristic dopaminergic cell firing pattern, and evidence of DA release (fig. S3, A to E).

To determine the effect of biallelic *SLC6A3* mutations on transporter function, we analyzed DAT activity in the DTDS neuronal cell model. Uptake of tritiated [^{3}H]dopamine in patient 1 and 2 lines was significantly reduced ($P = 0.0397$, $P = 0.0048$, respectively, and patient 2 versus CRISPR $P = 0.0033$), indicating a marked disruption of DAT activity (Fig. 1A). The impact of impaired transporter function on DA uptake and homeostasis was then evaluated by measurement of extracellular DA metabolites. High-performance liquid chromatography (HPLC) revealed significantly increased concentrations of HVA and 3,4-dihydroxyphenylacetic acid (DOPAC) ($P < 0.0001$, $P = 0.0002$, respectively, and patient 2 versus CRISPR $P = 0.0487$) (Fig. 1, B and C).

We sought to establish whether the observed loss of DAT function was secondary to reduced gene expression or impaired protein synthesis. There was no change in *SLC6A3* mRNA expression (fig. S4A), but increased DAT protein concentration was evident in patient-derived mDA neurons (Fig. 1D and fig. S4, B and C).

We then analyzed the impact of DAT dysfunction and dopaminergic dysregulation on other key enzymes involved in DA synthesis. Although patient-derived neuronal cultures showed an overall significant reduction in total tyrosine hydroxylase (TH) protein expression ($P = < 0.0001$ and $P = 0.0065$, respectively, and patient 2 versus CRISPR $P = 0.0238$) (Fig. 2A and fig. S5A), there were no differences in TH gene and protein expression specifically in the mDA neuronal subpopulation (Fig. 2B and fig. S5B). Furthermore, no differences in aromatic l-amino acid decarboxylase (AADC) mRNA and protein expression were found (Fig. 2, A and C, and fig. S5C).

In contrast, analysis of key enzymes involved in DA catabolism revealed a disease-specific reduction in monoamine oxidase A and B (MAO-A/B) gene and protein expression (Fig. 2, D to F, and fig. S5, D and E). In our neuronal cultures, MAO-A was widely expressed in both mDA neurons and glial cells (Fig. 2G) with significant reduction in MAO-A concentrations in patient-derived mDA neurons ($P = 0.0019$, $P = 0.0031$, respectively, and

patient 2 versus CRISPR $P = 0.0226$) (Fig. 2H). Unlike MAO-A, MAO-B expression was only detected in glial fibrillary acidic protein (GFAP)-positive cells (Fig. 2G), suggesting a disease-specific reduction of this enzyme in glial cells. We sought to determine whether aberrations in MAO-A and MAO-B were evident in CSF from patients with DTDS. Immunoblotting of patient CSF revealed no difference in MAO enzyme concentrations (fig. S5, F to H).

Impairment of DAT activity in DTDS is associated with neurotoxicity and apoptotic neurodegeneration

We identified a marked reduction of total neurons in patient-derived lines, compared to both age-matched and isogenic controls (Fig. 3, A and B, and fig. S6), and as a result, a proportionate patient-specific reduction of TH-positive cells (Fig. 3B and fig. S6). Apoptosis, as measured by cleaved caspase-3 (cCASP3) immuno-fluorescence, was significantly increased in neurons and more specifically in mDA neurons, but not in glial cells [microtubule-associated protein 2 (MAP2)/cCASP3/ 4′,6-diamidino-2-phenylindole (DAPI): $P = 0.0039$, $P = 0.0014$, respectively, and patient 2 versus CRISPR $P = 0.0013$; TH/cCASP3/DAPI: $P = 0.0025$, $P - 0.0001$, respectively, and patient 2 versus CRISPR $P < 0.0001$] (Fig. 3, and D, and fig. S7).

Further work was undertaken to elucidate potential mechanisms leading to apoptotic programmed cell death and neuronal loss. We first investigated the role of DA toxicity in DTDS pathogenesis as raised DA metabolites are observed in both patient CSF and the patient-derived neuronal cell model. Formation of carbonyl species, a marker of DA triggered stress response, was significantly increased in both DTDS patient-derived neuronal cultures and age-matched DA-treated controls, when compared to isogenic and DA-untreated controls (control versus control DA $P = < 0.0001$, $P = 0.0003$, $P = 0.0039$, and patient 2 versus CRISPR $P = 0.0292$) (Fig. 3, E and F).

Given the established pathogenic role of neuroinflammation in neurodegenerative disorders (16), we used the in vitro mDA model to investigate the effect of proinflammatory cytokines in the context of DA toxicity secondary to extracellular DA accumulation (17–19). Despite the presence of GFAP-positive glial cells in both patient- and control-derived neuronal cultures (Fig. 4A and fig. S8A), exposure to lipopolysaccharide (LPS) and DA did not induce cell death. There was no difference in cell membrane permeability in patient lines when compared to controls (Fig. 4B). Because of the relative immaturity of the glial system in our iPSC-derived mDA model, it is expected that we did not see LPS-stimulated cytokine release. We therefore artificially exposed our mDA neuronal model to the glial cell−derived proinflammatory cytokines, tumor necrosis factor−α (TNFα) and interleukin-1β (IL-1β), with and without the addition of DA. Whereas TNFα and IL-1β did not affect cell death per se, concurrent treatment with DA led to a disease-specific significant increase in membrane permeability and caspase-dependent cell death (TNFα: $P = 0.0314$ and $P = < 0.0001$, respectively; IL-1β: $P = < 0.0001$ and $P = 0.0029$, respectively) (Fig. 4, C and D).

Following these findings, we sought to determine whether there was evidence of proinflammatory cytokine release in DTDS by measuring cytokine concentrations in CSF of five patients. All had raised CSF HVA (mean CSF HVA:HIAA ratio of 10.8, normal range of

1.3 to 4.0) (20). Overall, there was no difference in TNF in patients with DTDS compared to pediatric controls (fig. S8B).

However, we identified raised TNF in two patients with more advanced disease (aged 6 and 16 years), in contrast to those with early stage disease ($n = 3$, all aged <2 years) (fig. S8C).

DAT function can be rescued with pifithrin-μ and lentiviral gene transfer in the patient-derived mDA neuronal model

Having established disease-specific parameters in the DTDS iPSC-derived mDA model, we used the model to validate targeted treatments for DTDS. Most missense variants in DTDS are associated with loss of transporter function, due to protein folding defects, retention in the endoplasmic reticulum (ER) (21–23), and reduced surface expression of mature glycosylated transporter (3–5). Therefore, we tested whether the heat shock protein 70 (HSP70) inhibitor pifithrin-μ could rescue defective protein folding and restore DAT function in vitro (21). Mature mDA neurons at day 65 were treated for 24 hours with pifithrin-μ, before measuring the uptake of tritiated DA. Neurons derived from patient 1 showed a significant twofold increase in DAT activity ($P = 0.0006$), reaching 35% of mean DA uptake activity observed in control lines with no overall increase in total DAT protein (Fig. 5A and fig. S9, A and B). No increase in DAT activity with pifithrin-μ was observed for patient 2 (Fig. 5A).

Given the mutation-specific effects of pifithrin-μ treatment, we sought to develop a gene therapy approach, applicable to a broader range of patients with DTDS. A lentiviral construct was generated expressing human *SLC6A3* gene under the transcriptional control of the neuron-specific promoter, human synapsin (hSYN1) (fig. S9, C and D). Patient-derived mDA precursors were transduced at day 24 of differentiation and analyzed at day 65 of derived maturity. Lentiviral gene transfer led to restoration of DA uptake (Fig. 5B). Despite this recovery of DAT activity, we did not observe normalization of dys-regulated MAO-A and MAO-B enzyme concentrations by day 65 (fig. S9, E to G). Nonetheless, rescue of DAT function by gene therapy successfully halted neuronal loss and, more specifically, prevented dopaminergic neurodegeneration (Fig. 5, C and D).

Proof-of-concept gene therapy of DAT knockout mice by neonatal intracerebroventricular gene transfer

In preparation for in vivo preclinical gene therapy, we injected adeno-associated virus serotype 9 (AAV9) vector encoding green fluorescent protein (GFP) under transcriptional control of a truncated hSyn1 promoter (fig. S10A) [2×10^{11} vector genomes (vg); $n = 4$, 1 male and 3 females from a single litter] into the lateral ventricle of neonatal wild-type mice. At 35 days, GFP expression extended bilaterally from the prefrontal cortex to cerebellum and was present in mDA neurons (fig. S10, B and C).

We established baseline phenotype readouts in a previously characterized DAT knockout mouse model (DAT-KO) (24, 25). Consistent with previous studies, all knockouts exhibited poor weight gain (Fig. 6A), displaying hyperlocomotor activity by postnatal day 21 (P21) (movie S1) with 59% developing tremor, bra-dykinesia, and weight loss (movie S2), reaching humane endpoint by P35 ($n = 10$, 4 males and 6 females) (Fig. 6B).

We generated an AAV9 vector for human DAT (hDAT) expression under transcriptional control of a truncated hSyn1 promoter (fig. S10D). At P0, DAT knockout pups received intrace-rebroventricular injection of vector (2.25×10^{10} vg per pup; $n = 13$, 7 males and 6 females from four litters). Uninjected wild-type littermates ($n = 12$, 5 males and 7 females from five litters) and knockouts ($n = 17$, 9 males and 8 females from seven litters) served as controls. Treated knockouts were significantly heavier than surviving untreated knockouts ($P = 0.001$) (Fig. 6A). Ten of 17 untreated knockouts required euthanization before 35 days; the remainder survived until tissue collection at 365 days. All treated knockouts and wild-type mice survived to the collection time points (Fig. 6B). Untreated knockouts were hyperactive, traveling significantly further distances (at 3, 6, 9, and 12 months; $P = < 0.0001$) and with less central zone time in open field tests ($P = < 0.0001$); treated knockouts were indistinguishable from wild-type littermates in both distance traveled and central time (Fig. 6, C and D). Knockouts had a significantly prolonged descent time on the vertical pole test (at 3, 6, 9, and 12 months; $P = < 0.0001$) and made significantly more foot faults (3 months, $P = < 0.0001$; 6 months, $P = 0.0015$; 9 months, $P = 0.0003$; 12 months, $P = < 0.0001$); the performance of treated knockouts was indistinguishable from wild-type mice (Fig. 6, E and F). Treated knockouts did not develop parkinsonism, unlike their untreated knockout littermates (movie S3).

Treated knockouts expressed hDAT bilaterally from the prefrontal cortex to cerebellum including striatum and midbrain, where DAT is physiologically expressed (Fig. 6G). Whole-brain homogenate from untreated knockouts had significantly reduced DA concentrations ($P = < 0.0001$) with raised DOPAC and HVA compared with wild-type mice; these differences were reversed, but not normalized, in treated knockouts (Fig. 6H). Gene therapy ameliorated both dopaminergic and striatal neurodegeneration (Fig. 6, I and J). Patch clamp electrophysiology of medium spiny neurons in the dorsal striatum revealed the presence of two different populations in wild-type mice, exhibiting high and low firing rates, and only high-firing rate neurons were detected in the untreated knockouts. AAV9.SLC6A3 treatment of knockouts restored the bimodal firing distribution (Fig. 6K and fig. S11) (χ^2 test, $P = 0.003$).

To attempt to fully restore DA homeostasis and neurotransmitter profile, a second knockout group received a 10-fold higher dosage of intracerebro-ventricular AAV9.SLC6A3 gene therapy at P0 (2.25×10^{11} vg per pup; $n = 12$, 7 males and 5 females from four litters) by injection. Treated mice were heavier than untreated knockouts; however, 50% of them developed unexpected early tremor, bradykinesia, and weight loss necessitating euthanasia by P35 (fig. S12, A and B). The remainder were indistinguishable, on motor behavioral testing, from wild-type and survived to euthanization at 365 days (fig. S12, C to F, and movie S4). Bilateral hDAT expression was observed throughout the brain; however, mDA transduction was not increased compared to lower dose cohort (fig. S12, G to I). Furthermore, despite restoration of HVA concentrations and correction of neurodegeneration (fig. S12, J to L), there was cortical cell loss and vacuolation with marked GFAP expression in the cerebral cortex (fig. S12M).

Preclinical gene therapy for DTDS-targeted delivery to the substantia nigra for future clinical translation

To move toward translation, we further developed vector delivery to model clinical application and restrict expression to dopaminergic neurons by intraparenchymal stereotactic delivery. We selected AAV2 capsid, which exhibits restricted spread after central nervous system delivery (26) and has precedent in gene therapy clinical trials of related disorders (27). Primary DAT knockout neurons treated with AAV2.SLC6A3 vector expressed hDAT protein and exhibited DA uptake as indicated by reduction of HVA concentration (fig. S13, A to D).

AAV2.SLC6A3 was delivered by bilateral stereotactic injection to the substantia nigra (SN) of 4-week-old symptomatic knockouts (modeling adolescent patients with DTDS) at three dosages: neat = 2×10^{10}, 1:10 = 2×10^{9}, and 1:100 = 2×10^{8} vg per mouse, respectively; $n = 8$ per group, 13 males and 11 females from six litters). AAV2.GFP control vector was injected to wild-type and knockout littermates (2×10^{10} vg per mouse; $n = 8$ per group, 7 males and 9 females from four litters) (fig. S14A). Growth was equivalent between groups (Fig. 7A). Survival was improved in all AAV2. SLC6A3-treated animals compared to AAV2.GFP-treated knockouts with 100% survival of the neat dosage group at 12 weeks of age (Fig. 7B). With the lowest dosage (2×10^{8} vg per mouse), one mouse developed weight loss and parkinsonism, surviving at P50. Three of eight (37.5%) AAV2.GFP-treated knockouts reached humane endpoint at 5, 6, and 8 weeks. At 8 weeks ($n = 5$ to 8 per group), knockouts treated with highest dosage (2×10^{10} vg per mouse) displayed motor behavior that was indistinguishable from AAV2.GFP-treated wild-types (Fig. 7, C to F, fig. S14B, and movie S5). Dose response was observed in open field distance traveled and central time (Fig. 7, C and D, fig. S14B, and movie S6). Vertical pole descent time was restored to wild-type times in 2×10^{10} and 2×10^{9} vg per mouse but not the lowest dosage (2×10^{8} vg/mouse), and percentage of foot faults were restored to wild-type rates in all treated knockouts (Fig. 7, E and F). hDAT staining in midbrain and striatum confirmed midbrain expression with dose-dependent anterograde transport to the striatum (Fig. 7G). Quantification of TH-positive mDA neurons expressing hDAT showed rescue of neurodegeneration (Fig. 7, H and I) correlating with midbrain TH transduction, hDAT mRNA transcripts, and vector genome copies delivered (Fig. 7H and fig. S14, C to E). Consistent with iPSC-derived mDA, knockouts had significantly lower MAO-A and MAO-B in the midbrain versus wild-type ($P = 0.02$ and 0.001, respectively) (fig. S14, F and G). Treatment with AAV2.SLC6A3 neat dosage significantly increased but did not normalize these enzymes (MAO-A, $P = 0.03$ and MAO-B, $P = 0.02$) (fig. S14, F and G). With targeted stereotactic SN delivery, cortical cell loss or vacuolation was not observed (Fig. 7J).

Discussion

Personalized medicine strategies are increasingly important in drug development, particularly for inherited neurodegenerative disorders, where the mainstay of current treatment is symptom control and palliative care. Through the synergistic use of iPSC-derived neuronal and mouse models, we have obtained further insight into the underlying mechanisms governing human disease and have evaluated potential therapeutic

strategies for this pharmacoresistant condition. Both models recapitulate important DTDS disease features, with loss of DAT activity, abnormally raised DA metabolites, and neurodegeneration. The mouse model exhibits key motor features of human patients, with early hyperkinesia evolving into late-stage parkinsonism. Previous studies of DTDS missense variants (which account for 76.6% of DTDS patient mutations) have used cell-based overexpression models, *Caenorhabditis elegans* and *Drosophila melanogaster* DAT mutants (3–5, 22, 23, 28). Our iPSC-based platform provides a DTDS model with a number of advantages: it allows the study of patient-relevant DAT mutations in a human-derived neuronal model system, including variants that cannot be studied in other models such as L368Q, which confers lethality in the fly model (23). By combining the iPSC and murine disease-relevant models, we have gained further pathophysiological insight into the consequences of the loss of DAT function. Both the mDA cell model and knockout murine dissected midbrain show substantial reduction of key enzymes in DA catabolism, MAO-A and MAO-B, suggesting a compensatory down-regulation in the absence of DA reuptake. Dysregulation of MAO-A and MOA-B was not evident in patient CSF; however, CSF measurement likely does not represent midbrain MAO-A/MAO-B enzyme concentrations. Despite extensive phenotypic rescue of both iPSC and mouse models by gene therapy, restoration of DAT activity did not fully restore midbrain MAO enzyme concentrations. These studies reflect that MAO regulation is not solely influenced by DA reuptake. In the knockout mouse model, we also observed loss of the normal bimodal firing pattern in the medium spiny neuron population, suggesting that DAT deficiency in mDA neurons may have more widespread detrimental systemic effects on synaptic connectivity and postsynaptic neuronal networks.

iPSC-derived mDA neurons and knockouts exhibit neurodegeneration. Although there is limited evidence in patient with DTDS, the progressive nature of clinical disease (4, 5, 7) and serial DaTscan imaging (7) also both point to a neurodegenerative process. From the iPSC-derived mDA model, we postulate that neuronal loss is mediated by an oxidative stress response, secondary to extracellular DA toxicity, with proinflammatory cytokine-induced apoptosis. This is corroborated by our findings of raised TNF in CSF of older patients with DTDS with more advanced disease. Overall, it is likely that the mechanisms governing neurodegeneration in DTDS are multifactorial; apoptosis may be driven by factors such as DA toxicity and oxidative stress, possibly accelerated by the release of pro-inflammatory cytokines from activated glia.

Our study highlights the therapeutic limitations of agents such as pifithrin-μ with its mutation-specific chaperone effects (21–23) and, in contrast, the wider potential of gene therapy for all patients with DTDS, showing clear evidence of phenotypic rescue in both the cell and knockout mouse model. In the absence of a humanized knock-in mouse, our iPSC-derived model provides potentially clinically relevant information regarding potential dominant-negative phenomena. Antagonistic effects from coexpression of both the endogenous mutant allele and wild-type transgene were not observed in the lentivirus-treated cells.

From our study, it is clear that the neuropathological consequences of DTDS are likely to occur early in life. It is universally acknowledged that despite the maturation process, iPSC-

derived neurons resemble fetal neurons and the severe cellular phenotype evident in our DTDS mDA cell model suggests prenatal disease onset. The knockout mouse corroborates this, where poor growth and an early progressive motor phenotype with neuronal loss is observed. AAV vectors have been used successfully for clinical translation of targeted intraparenchymal gene therapy in other similar early-onset neurotransmitter disorders (27, 29) and hence would be a logical approach to pursue for DTDS, given our highly promising in vivo preclinical data.

We initially sought to explore neonatal gene therapy, given its therapeutic potential for this early onset neurodegenerative disease; the youngest patients benefited most in recent gene therapy clinical trials for spinal muscular atrophy (30) and mucopolysaccharidosis type IIIA (31). Despite variable gene expression in target mDA neurons, our neonatal gene therapy in knockouts prevented early demise, normalized motor function, and restored DAT activity and DA homeostasis. Neuronal loss from the SN was prevented, and beneficial effects on the postsynaptic neuronal network included prevention of neuronal loss and normalization of electrophysiological properties of the medium spiny neuron population. Although there was off-target transduction, ectopic overexpression of DAT appeared to be well tolerated. However, at a 10-fold higher vector dose, we observed off-target neurotoxicity with astrogliosis in cortical regions and substantial reduction in survival. Neurotoxic effects and reduced survival have been similarly observed in DAT overexpression and ectopic expression transgenic models (32, 33). Overall, this strongly suggests that, although low ectopic expression is tolerated, it should ideally be avoided for clinical translatability.

The study of Illiano *et al.* (34) provided a proof of concept for gene therapy of DAT deficiency. They delivered two AAV vectors into the midbrain of adult DAT mice by stereotactic injection. To achieve high specificity for dopaminergic neurons, the first AAV expressed Cre recombinase under the control of the truncated rat TH promoter and a second AAV contained murine DAT flanked by loxP sites, under the control of a constitutive CMV promoter. Cre recombinase expression thus permitted specific therapeutic DAT expression. Despite this proof of concept, such an approach would not be clinically translatable, with the use of murine DAT and potential neurotoxicity of Cre recombinase expression (35).

Because both neonatal intracerebroventricular gene delivery (with risk of potential neurotoxic off-target effects) and the dual AAV vector delivery system described above (with neurotoxic Cre recombinase) are unsuitable for clinical translation, we developed a potentially clinically applicable gene therapy approach for patients with DTDS using AAV2 vector, stereotactically targeted to the DAT-expressing SN of the brain. We demonstrated the efficacy of the therapeutic expression cassette containing a truncated human promoter and human *SLC6A3* cDNA, in vitro in the patient-derived dopaminergic neuronal cell model, primary knockout neurons, and in vivo at different developmental ages of the knockout mouse model. Crucially for clinical translation, we have also demonstrated potential clinical feasibility with a 2 log dose-ranging study of AAV2.SLC6A3 showing clear (dose-dependent) therapeutic efficacy with no evidence of neurotoxicity that might arise from ectopic hDAT expression.

This study was limited to patient-derived iPSC cell lines and a mouse model in which the m*SLC6A3* gene was disrupted. Dopaminergic neurotransmission across a functioning synapse was not assessed using this presynaptic iPSC model. However, it would be fascinating to do so using organotypic cultures, brain organoids, or in vivo optogenetic techniques (36). Some question whether the knockout mouse is a sufficient model for studying cognitive behavioral processes to study neuropsychiatric conditions, prompting the generation of rat models carrying disruptions in the DAT gene (37). It would be interesting to assess therapeutic efficacy of AAV. SLC6A3 on behavioral parameters representing each of the five research domain criteria as previously evaluated in one of these models (38). Although the promising experimental data presented here will advance efforts toward clinical trial, it is important that preclinical studies are repeated to obtain long-term readouts, up to a year, of efficacy and to evaluate any evidence of toxicity arising from possible expression of hDAT in nondopaminergic neurons. Additional challenges relating to human translation are worthy of discussion; for such precision medicine approaches to be effective, there is a need for accurate neurosurgical targeting, which requires considerable expertise and optimal vector dosing to maximize efficacy and avoid neurotoxicity. A clear understanding of the disease is also necessary to ensure that the most suitable patients are put forward for trial, potentially determined by genotype, age, and disease stage for optimum therapeutic time window. One potential modification to improve safety and efficacy could be to use a dopaminergic neuron-specific promoter, although the difficulty in identifying a translatable dopaminergic neuron-specific promoter is widely acknowledged in the field. Studies of truncated human TH promoters have shown low to high promoter strength with variable specificity (36). These TH promoters have not been used clinically and are unlikely to improve our vector efficacy, safety, and translatability. Moreover, the current gene therapy trials for related disorders such as AADC deficiency (NCT01395641 and NCT01973543) used the AAV2 capsid with a ubiquitous promoter, combined with stereotactic delivery to successfully target specific brain regions such as the striatum and midbrain with marked patient benefit (39–42). Our use of hSyn promoter improves neuronal selectivity in comparison, and the efficacy and safety achieved through our vector design and delivery method clearly supports future translation of our approach toward a clinical trial of AAV gene therapy for patients with DTDS.

Materials And Methods

Study design

The aim of this study was to (i) understand the mechanisms underpinning DTDS in an in vitro patient-derived mDA model and (ii) develop a gene therapy strategy to rescue disease in vitro and in vivo.

For the generation of a patient-derived neuronal model, we obtained fibroblasts from patients and reprogrammed them into iP-SCs. To rule out the effect of genetic background, we generated an isogenic control iPSC line with correction of the disease-associated homozygous *SLC6A3* mutation. A tritiated DA uptake assay and HPLC were performed to confirm DAT dysfunction in mature derived mDA neurons. We then investigated cellular disease mechanisms by immunoblotting, quantitative reverse transcription polymerase

Europe PMC Funders Author Manuscripts

chain reaction (qRT-PCR), and immunofluorescence analysis, identifying disease-specific dysregulation of DA metabolites and neurodegenerative processes. A cell viability assay was performed on the mDA cultures to investigate inflammatory response and an enzyme-linked immunosorbent assay on patient CSF to investigate proinflammatory cytokine release. We then developed a lentiviral-based gene therapy delivery approach and analyzed DAT activity and markers of neurodegeneration after gene transfer.

For reproducibility and reliability of our dataset, we have used standardized protocols and performed blinded analyses, except in Figs. 3D and 5D and fig. S2B. The number of replications of each independent experiment is reported in the respective figure legends. Single experiments, which failed for technical reasons, have been selectively discarded from the analysis. Tritiated DA uptake assays of untreated (Fig. 1A) and pifithrin-μ–treated (Fig. 5A) lines have been performed simultaneously to avoid technical variability, and as such, they partially share the same dataset for untreated samples.

The in vivo studies were designed to test the hypothesis that AAV-mediated gene therapy would restore DAT function in the knockout mouse model of DTDS. We evaluated the efficacy of neonatal AAV9-mediated gene transfer with endpoints of survival, locomotor behavior, and neurotransmitter analysis. We assessed toxicity related to dosage and off-target expression and then delivered gene therapy to adult knockout mice with AAV2 capsid by stereotactic injection with the same endpoints. The number of biological replicates varied between studies (n = 5 to 17) and is indicated in the figure legends. Animals were randomly assigned to the vector treatment group. Assessment of outcomes was blinded through labeling without treatment information on behavioral analysis videos, tissue samples for biodistribution, and pathological analysis.

Statistical analysis

Statistical analysis tailored to each experiment was performed using GraphPad Prism version 8. For the statistical analysis of iPSC-derived data, when dual comparisons were required, two-tailed Student's t test was applied, whereas for multiple comparisons, one-way analysis of variance (ANOVA) was performed. In vivo experimental design and sample sizes were designed using NC3Rs guidance and power calculation. For most analyses of animal experiments, one-way or two-way ANOVA was performed with either Bonferroni or Tukey's multiple comparison test. Percentage of foot faults was converted by log transformation before ANOVA. For neuronal firing, Kruskal-Wallis distribution and χ^2 tests were applied.

Supplementary Material

Refer to Web version on PubMed Central for supplementary material.

Acknowledgments

We sincerely thank our patients and their families for participating in this study. We thank UCL Genomics (UCL GOS-Institute of Child Health) for undertaking single-nucleotide polymorphism microarray studies. This research was supported by the NIHR Great Ormond Street Hospital Biomedical Research Centre. The views expressed are those of the author(s) and not necessarily those of the NHS, the NIHR, or the Department of Health. We thank GOS-Institute of Child Health Biomedical Research Centre for support in statistical analysis and the MRC Centre

for Neuromuscular Disorders Biobank for providing age-matched control fibroblasts. We thank V. Leuzzi and B. B. Zeev for providing patient fibroblasts and H. Sampaio, S. Bandodkar, R. Artuch, and A. A. Mathew for providing patient CSF toward this study. We thank M. G. Caron, R. R. Gainetdinov, and W. Roberts for support with the mouse transgenic colony. We thank L. Gianfrancesco for proofreading the manuscript.

Funding

This research was supported through Wellcome Intermediate Clinical Fellowship (WT098524MA to M.A.K. and S.B.), UK Medical Research Council (MRC) Clinical Research training fellowship (MR/K02342X/1 to J.N.), MRC Biomedical Catalyst Developmental Pathway Funding Scheme (MR/R015325/1 to S.N.W., M.A.K., A.A.R., and J.N.), Great Ormond Street Hospital Children's Charity and the Rosetrees Trust, Robert Luff Foundation and John Black Foundation (V1284 and M576 to M.A.K., J.N., and S.N.W.), NIHR Research Professorship (NIHR-RP-2016-07-019 to M.A.K.), Sir Jules Thorn Award for Biomedical Research (to M.A.K.), Marie Skłodowska-Curie Actions of the European Union's Seventh Framework Programme FP7 under REA grant agreement for "Training in Neurodegeneration, Therapeutics, Intervention and Neurorepair" (608381 to C.D.L.F.B.), Epilepsy Research UK F1701 Marie Curie Fellowship (658418 to G.L.), Joan Pitts-Tucker/Moritz studentship (to R.W.), and UCL IMPACT PhD studentship (to R.P.). H.A. is funded by the Kuwait University. This work was also supported by the Monument Trust Discovery Award from Parkinson's UK (Grant J-1403 to R.W.-M., J.V., and S.A.C.); the National Institute for Health Research (544454 to G.R.); MRC, Sparks, LifeArc, and Great Ormond Street Children's Charity and Dravet Syndrome UK (MR/P026494/1, 17UCL01, P2020-0008, and V4720 to R.K., S. Schorge, and S.N.W.); MRC (MR/N019075/1 to D.P. and J.B.); Action Medical Research for Children Charity Nutricia Metabolic Research Grant (GN2137 to J.B.); London Advanced Therapy/Confidence in Collaboration (2CiC017, MRC MR/T008024/1 to J.B.); Wellbeing of Women fellowship (RT-414 to N.S.); CONICYT Becas Chile Doctoral Fellowship Program (72160294 to J.A.D.); LifeArc (P2020-0008 to J.A.D.); the Royal Society (UF140596 to S. Schorge); Versus Arthritis (PhD scholarship 21552 and grant 21593 to L.R.M.); Austrian Science Fund FWF (P31255-B27 to S. Sucic) and Vienna Science and Technology Fund WWTF (LSC17-026 to M.F.); Wellcome Innovator Award (21077/Z/18/Z to J.R.C.); Muscular Dystrophy UK and Association Française contre les myopathies (Translamuscle program, project 19507 and 22946 to M.B.); MRC (MR/N026101/1 to A.A.R. and S.N.W., and MR/R025134/1, MR/S009434/1, MR/S036784/1, and MR/T044853/1 to A.A.R.); NC3Rs (NC/L001780/1 to A.A.R. and S.N.W.); Wellcome Trust Institutional Strategic Support Fund/UCL Therapeutic Acceleration Support (TAS) Fund (204841/Z/16/Z to A.A.R.); European Union's Horizon 2020 research and innovation program under grant agreement no. 666918 (BATCure to A.A.R.); and Action Medical Research (GN2485 to A.A.R.). A.A.R. is supported by the UK Gauchers Association, Asociación Niemann Pick de Fuenlabrada, and NIHR GOSH BRC (the views expressed are those of the author(s) and not necessarily those of the NHS, the NIHR, or the Department of Health).

Data and materials availability

All data associated with study are available in main text or the Supplementary Materials.

References

1. Poewe W, Seppi K, Tanner CM, Halliday GM, Brundin P, Volkmann J, Schrag A-E, Lang AE. Parkinson disease. Nat Rev Dis Primers. 2017; 3 17013 [PubMed: 28332488]
2. Massaro G, Mattar CNZ, Wong AMS, Sirka E, Buckley SMK, Herbert BR, Karlsson S, Perocheau DP, Burke D, Heales S, Richard-Londt A, et al. Fetal gene therapy for neurodegenerative disease of infants. Nat Med. 2018; 24: 1317–1323. [PubMed: 30013199]
3. Kurian MA, Zhen J, Cheng S-Y, Li Y, Mordekar SR, Jardine P, Morgan NV, Meyer E, Tee L, Pasha S, Wassmer E, et al. Homozygous loss-of-function mutations in the gene encoding the dopamine transporter are associated with infantile parkinsonism-dystonia. J Clin Invest. 2009; 119: 1595–1603. [PubMed: 19478460]
4. Kurian MA, Li Y, Zhen J, Meyer E, Hai N, Christen H-J, Hoffmann GF, Jardine P, von Moers A, Mordekar SR, O'Callaghan F, et al. Clinical and molecular characterisation of hereditary dopamine transporter deficiency syndrome: An observational cohort and experimental study. Lancet Neurol. 2011; 10: 54–62. [PubMed: 21112253]

5. Ng J, Zhen J, Meyer E, Erreger K, Li Y, Kakar N, Ahmad J, Thiele H, Kubisch C, Rider NL, Morton DH, et al. Dopamine transporter deficiency syndrome: Phenotypic spectrum from infancy to adulthood. Brain. 2014; 137: 1107–1119. [PubMed: 24613933]
6. Torres GE, Gainetdinov RR, Caron MG. Plasma membrane monoamine transporters: Structure, regulation, and function. Nat Rev Neurosci. 2003; 4: 13–25. [PubMed: 12511858]
7. Hansen FH, Skjørringe T, Yasmeen S, Arends NV, Sahai MA, Erreger K, Andreassen TF, Holy M, Hamilton PJ, Neergheen V, Karlsborg M, et al. Missense dopamine transporter mutations associate with adult parkinsonism and ADHD. J Clin Invest. 2014; 124: 3107–3120. [PubMed: 24911152]
8. Yildiz Y, Pektas E, Tokatli A, Haliloglu G. Hereditary dopamine transporter deficiency syndrome: Challenges in diagnosis and treatment. Neuropediatrics. 2017; 48: 49–52. [PubMed: 27690368]
9. Kuster A, Arnoux J-B, Barth M, Lamireau D, Houcinat N, Goizet C, Doray B, Gobin S, Schiff M, Cano A, Amsallem D, et al. Diagnostic approach to neurotransmitter monoamine disorders: Experience from clinical, biochemical, and genetic profiles. J Inherit Metab Dis. 2018; 41: 129–139. [PubMed: 28924877]
10. Galiart A, Weber P, Datta AN. Infantile dystonia parkinsonism caused by mutations in SLC6A3: Case report of three siblings. Neuropediatrics. 2017; 48: S1–S45.
11. Heidari E, Razmara E, Hosseinpour S, Tavasoli AR, Garshasbi M. Homozygous in-frame variant of SCL6A3 causes dopamine transporter deficiency syndrome in a consanguineous family. Ann Hum Genet. 2020; 84: 315–323. [PubMed: 32077500]
12. Baga M, Spagnioli C, Soliano L, Salerno GG, Rizzi S, Frattini D, Pisani F, Fusco C. Early-onset dopamine transporter deficiency syndrome: Long-term follow-up. Can J Neurol Sci. 2021; 48: 285–286. [PubMed: 32646530]
13. Nasehi MM, Nikkah A, Salari M, Soltani P, Shirzadi S. Dopamine transporter deficiency syndrome: A case with hyper- and hypokinetic extremes. Mov Disord Clin Pract. 2020; 7: S57–S60. [PubMed: 33015223]
14. Kirkeby A, Grealish S, Wolf DA, Nelander J, Wood J, Lundblad M, Lindvall O, Parmar M. Generation of regionally specified neural progenitors and functional neurons from human embryonic stem cells under defined conditions. Cell Rep. 2012; 1: 703–714. [PubMed: 22813745]
15. Lehnen D, Barral S, Cardoso T, Grealish S, Heuer A, Smiyakin A, Kirkeby A, Kollet J, Cremer H, Parmar M, Bosio A, et al. IAP-based cell sorting results in homogeneous transplantable dopaminergic precursor cells derived from human pluripotent stem cells. Stem Cell Rep. 2017; 9: 1207–1220.
16. Ransohoff RM. How neuroinflammation contributes to neurodegeneration. Science. 2016; 353: 777–783. [PubMed: 27540165]
17. Sochocka M, Diniz BS, Leszek J. Inflammatory response in the CNS: Friend or foe? Mol Neurobiol. 2017; 54: 8071–8089. [PubMed: 27889895]
18. He Q, Wang Q, Yuan C, Wang Y. Downregulation of miR-7116-5p in microglia by MPP^+ sensitizes TNF-α production to induce dopaminergic neuron damage. Glia. 2017; 65: 1251–1263. [PubMed: 28543680]
19. Sanchez-Guajardo V, Tentillier N, Romero-Ramos M. The relation between α-synuclein and microglia in Parkinson's disease: Recent developments. Neuroscience. 2015; 302: 47–58. [PubMed: 25684748]
20. Hyland K, Surtees RAH, Heales SJR, Bowron A, Howells DW, Smith I. Cerebrospinal fluid concentrations of pterins and metabolites of serotonin and dopamine in a pediatric reference population. Pediatr Res. 1993; 34: 10–14. [PubMed: 7689195]
21. Kasture A, El-Kasaby A, Szöllősi D, Asjad HMM, Grimm A, Stockner T, Hummel T, Freissmuth M, Sucic S. Functional rescue of a misfolded *Drosophila melanogaster* dopamine transporter mutant associated with a sleepless phenotype by pharmacological chaperones. J Biol Chem. 2016; 291: 20876–20890. [PubMed: 27481941]
22. Beerepoot P, Lam VM, Salahpour A. Pharmacological chaperones of the dopamine transporter rescue dopamine transporter deficiency syndrome mutations in heterologous cells. J Biol Chem. 2016; 291: 22053–22062. [PubMed: 27555326]
23. Asjad HMM, Kasture A, El-Kasaby A, Sackel M, Hummel T, Freissmuth M, Sucic S. Pharmacochaperoning in a *Drosophila* model system rescues human dopamine transporter variants

associated with infantile/juvenile parkinsonism. J Biol Chem. 2017; 292: 19250–19265. [PubMed: 28972153]

24. Giros B, Jaber M, Jones SR, Wightman RM, Caron MG. Hyperlocomotion and indifference to cocaine and amphetamine in mice lacking the dopamine transporter. Nature. 1996; 379: 606–612. [PubMed: 8628395]
25. Cyr M, Beaulieu J-M, Laakso A, Sotnikova TD, Yao W-D, Bohn LM, Gainetdinov RR, Caron MG. Sustained elevation of extracellular dopamine causes motor dysfunction and selective degeneration of striatal GABAergic neurons. Proc Natl Acad Sci USA. 2003; 100: 11035–11040. [PubMed: 12958210]
26. Murlidharan G, Samulski RJ, Asokan A. Biology of adeno-associated viral vectors in the central nervous system. Front Mol Neurosci. 2014; 7: 76. [PubMed: 25285067]
27. Hwu W-L, Muramatsu S-i, Tseng S-H, Tzen K-Y, Lee N-C, Chien Y-H, Snyder RO, Byrne BJ, Tai C-H, Wu R-M. Gene therapy for aromatic l-amino acid decarboxylase deficiency. Sci Transl Med. 2012; 4 134ra61
28. Illiano P, Lanzo A, Leo D, Paglione M, Zampi G, Gainetdinov RR, Di Schiavi E. A *Caenorhabditis elegans* model to study dopamine transporter deficiency syndrome. Eur J Neurosci. 2017; 45: 207–214. [PubMed: 27519790]
29. Chien Y-H, Lee N-C, Tseng S-H, Tai C-H, Muramatsu S-I, Byrne BJ, Hwu W-L. Efficacy and safety of AAV2 gene therapy in children with aromatic l-amino acid decarboxylase deficiency: An open-label, phase 1/2 trial. Lancet Child Adolesc Health. 2017; 1: 265–273. [PubMed: 30169182]
30. Mendell JR, Al-Zaidy S, Shell R, Arnold WD, Rodino-Klapac LR, Prior TW, Lowes L, Alfano L, Berry K, Church K, Kissel JT, et al. Single-dose gene replacement therapy for spinal muscular atrophy. N Engl J Med. 2017; 377: 1713–1722. [PubMed: 29091557]
31. Tardieu M, Zérah M, Husson B, de Bournonville S, Deiva K, Adamsbaum C, Vincent F, Hocquemiller M, Broissand C, Furlan V, Ballabio A, et al. Intracerebral administration of adeno-associated viral vector serotype rh.10 carrying human SGSH and SUMF1 cDNAs in children with mucopolysaccharidosis type IIIA disease: Results of a phase I/II trial. Hum Gene Ther. 2014; 25: 506–516. [PubMed: 24524415]
32. Masoud ST, Vecchio LM, Bergeron Y, Hossain MM, Nguyen LT, Bermejo MK, Kile B, Sotnikova TD, Siesser WB, Gainetdinov RR, Wightman RM, et al. Increased expression of the dopamine transporter leads to loss of dopamine neurons, oxidative stress, and L-DOPA reversible motor deficits. Neurobiol Dis. 2015; 74: 66–75. [PubMed: 25447236]
33. Chen L, Ding Y, Cagniard B, Van Laar AD, Mortimer A, Chi W, Hastings TG, Kang UJ, Zhuang X. Unregulated cytosolic dopamine causes neurodegeneration associated with oxidative stress in mice. J Neurosci. 2008; 28: 425–433. [PubMed: 18184785]
34. Illiano P, Bass CE, Fichera L, Mus L, Budygin EA, Sitnikova TD, Leo D, Espinoza S, Gainetdinov RR. Recombinant adeno-associated virus–mediated rescue of function in a mouse model of dopamine transporter deficiency syndrome. Sci Rep. 2017; 7 46280 [PubMed: 28417953]
35. Amin SR, Gruszczynski C, Guiard BP, Callebert J, Launay J-M, Louis F, Betancor C, Vialou V, Gautron S. Viral vector-mediated Cre recombinase expression in substantia nigra induces lesions of the nigrostriatal pathway associated with perturbations of dopamine-related behaviors and hallmarks of programmed cell death. J Neurochem. 2019; 150: 330–340. [PubMed: 30748001]
36. Liu C, Kershberg L, Wang J, Schneeberger S, Kaeser PS. Dopamine secretion is mediated by sparse active zone–like release sites. Cell. 2018; 172: 706–718. e15 [PubMed: 29398114]
37. Leo D, Sukhanov I, Zoratto F, Illiano P, Caffino L, Sanna F, Messa G, Emanuele M, Esposito A, Dorofeikova M, Budygin EA, et al. Pronounced hyperactivity, cognitive dysfunctions, and BDNF dysregulation in dopamine transporter knock-out rats. J Neurosci. 2018; 38: 1959–1972. [PubMed: 29348190]
38. Vengeliene V, Bespalov A, Roßmanith M, Horschitz S, Berger S, Relo AL, Noori HR, Schneider P, Enkel T, Bartsch D, Schneider M, et al. Towards trans-diagnostic mechanisms in psychiatry: Neurobehavioral profile of rats with a loss-of-function point mutation in the dopamine transporter gene. Dis Model Mech. 2017; 10: 451–461. [PubMed: 28167616]

39. Rolland A-S, Kareva T, Yarygina O, Kholodilov N, Burke RE. Expression mediated by three partial sequences of the human tyrosine hydroxylase promoter in vivo. Mol Ther Methods Clin Dev. 2016; 3 16062 [PubMed: 27689101]
40. Christine CW, Bankiewicz KS, Van Laar AD, Richardson RM, Ravina B, Kells AP, Boot B, Martin AJ, Nutt J, Thompson ME, Larson PS. Magnetic resonance imaging-guided phase 1 trial of putaminal AADC gene therapy for Parkinson's disease. Ann Neurol. 2019; 85: 704–714. [PubMed: 30802998]
41. Palfi S, Gurruchaga JM, Ralph GS, Lepetit H, Lavisse S, Buttery PC, Watts C, Miskin J, Kelleher M, Deeley S, Iwamuro H, et al. Long-term safety and tolerability of ProSavin, a lentiviral vector-based gene therapy for Parkinson's disease: A dose escalation, open-label, phase 1/2 trial. Lancet. 2014; 383: 1138–1146. [PubMed: 24412048]
42. San Sebastian W, Kells AP, Bringas J, Samaranch L, Hadaczek P, Ciesielska A, Macayan MJ, Pivirotto PJ, Forsayeth J, Osborne S, Wright JF, et al. Safety and tolerability of MRI-guided infusion of AAV2-AADC into the mid-brain of nonhuman primate. Mol Ther Methods Clin Dev. 2014; 3 14049 [PubMed: 25541617]
43. Lenz M, Goetzke R, Schenk A, Schubert C, Veeck J, Hemeda H, Koschmieder S, Zenke M, Schuppert A, Wagner W. Epigenetic biomarker to support classification into pluripotent and non-pluripotent cells. Sci Rep. 2015; 5: 8973. [PubMed: 25754700]
44. Reith MEA, Xu C, Carroll FI, Chen N-H. Inhibition of [^{3}H]dopamine translocation and [^{3}H]cocaine analog binding: A potential screening device for cocaine antagonists. Methods Enzymol. 1998; 296: 248–259. [PubMed: 9779453]
45. de la Fuente C, Burke DG, Eaton S, Heales SJR. Inhibition of neuronal mitochondrial complex I or lysosomal glucocerebrosidase is associated with increased dopamine and serotonin turnover. Neurochem Int. 2017; 109: 94–100. [PubMed: 28242245]
46. Kügler S, Kilic E, Bähr M. Human synapsin 1 gene promoter confers highly neuronspecific long-term transgene expression from an adenoviral vector in the adult rat brain depending on the transduced area. Gene Ther. 2003; 10: 337–347. [PubMed: 12595892]
47. Dull T, Zufferey R, Kelly M, Mandel RJ, Nguyen M, Trono D, Naldini L. A third-generation lentivirus vector with a conditional packaging system. J Virol. 1998; 72: 8463–8471. [PubMed: 9765382]
48. Charrier S, Ferrand M, Zerbato M, Précigout G, Viornery A, Bucher-Laurent S, Benkhelifa-Ziyyat S, Merten OW, Perea J, Galy A. Quantification of lentiviral vector copy numbers in individual hematopoietic colony-forming cells shows vector dose-dependent effects on the frequency and level of transduction. Gene Ther. 2011; 18: 479–487. [PubMed: 21160533]
49. Binny CJ, Nathwani AC. Vector systems for prenatal gene therapy: Principles of adeno-associated virus vector design and production. Methods Mol Biol. 2012; 891: 109–131. [PubMed: 22648770]
50. Kim J-Y, Grunke SD, Levites Y, Golde TE, Jankowsky JL. Intracerebroventricular viral injection of the neonatal mouse brain for persistent and widespread neuronal transduction. J Vis Exp. 2014. e51863
51. Paxinos, G, Franklin, K. Paxinos and Franklin's the Mouse Brain in Stereotaxic Coordinates. Academic Press; 2012. 360
52. Rahim AA, Wong AMS, Hoefer K, Buckley SMK, Mattar CN, Cheng SH, Chan JKY, Cooper JD, Waddington SN. Intravenous administration of AAV2/9 to the fetal and neonatal mouse leads to differential targeting of CNS cell types and extensive transduction of the nervous system. FASEB J. 2011; 25: 3505–3518. [PubMed: 21746868]

Europe PMC Funders Author Manuscripts

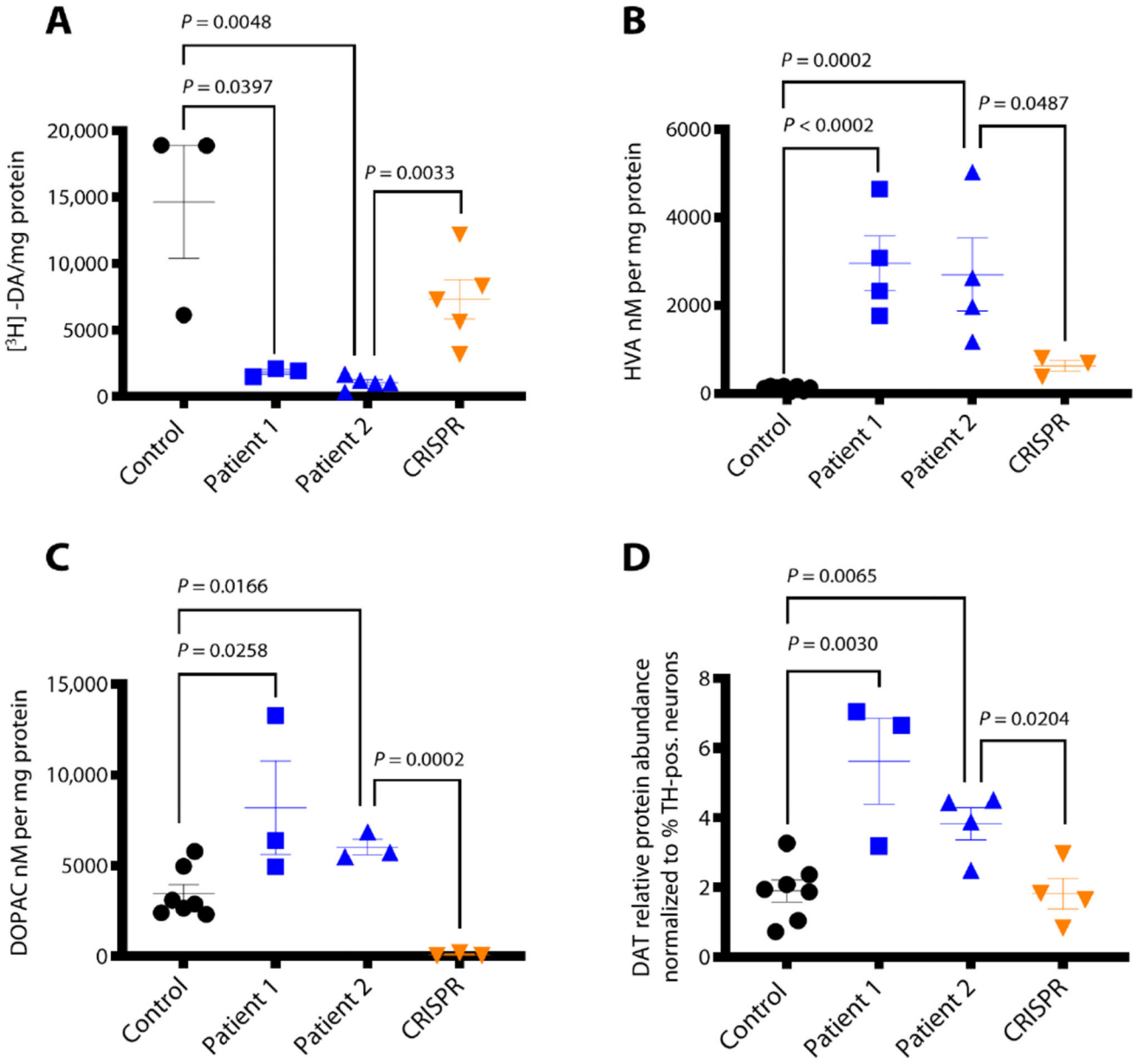

Fig. 1. DTDS-patient derived mDA neurons recapitulate key disease features.

(**A**) [^{3}H]dopamine uptake measured at day 65. Values are relative to protein concentration (n = 3, 3, 5, and 5 for control, patient 1, patient 2, and CRISPR, respectively). (**B** and **C**) HPLC detection of extracellular HVA and DOPAC at day 65 (n = 8, 4, 4, and 3, respectively, and n = 7, 3, 3, and 3, respectively). (**D**) Quantification of DAT protein detected in day 65 neurons derived from control, patient 1, patient 2, and CRISPR lines, relative to glyceraldehyde-3-phosphate dehydrogenase (GAPDH) and normalized to percentage of TH-positive cells in each neuronal population as reported in Fig. 3B (n = 7, 3, 4, and 4, respectively). Error bars indicate SEM. Both DTDS lines were independently compared to controls using two-tailed Student's t test for all analyses.

Europe PMC Funders Author Manuscripts

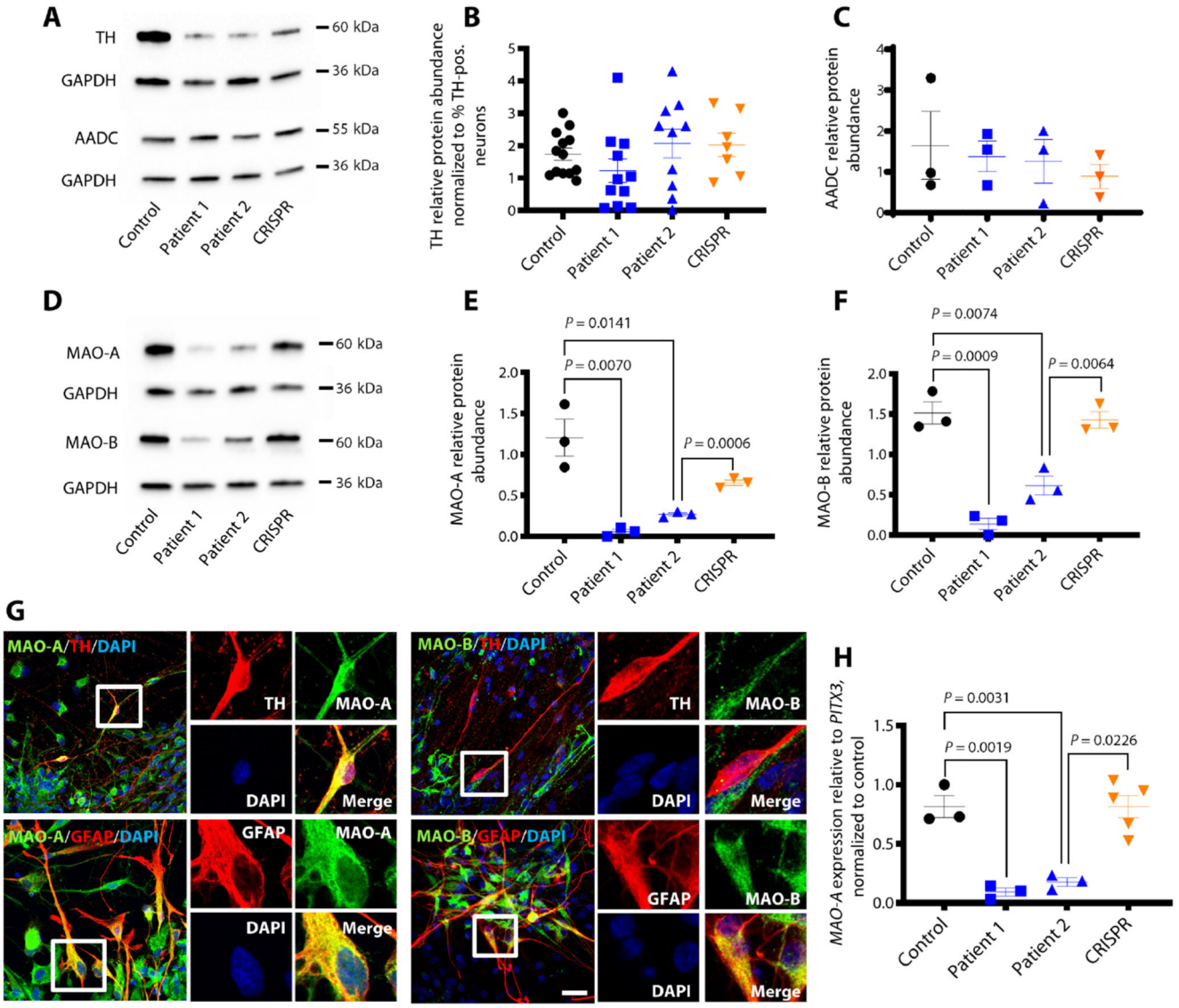

Fig. 2. DTDS-patient derived mDA neurons show dysregulation of key enzymes involved in DA catabolism.

(**A**) Cropped immunoblot of total TH protein and AADC detected at day 65. (**B**) Relative abundance of TH protein detected at day 65 in control, patient 1, patient 2, and CRISPR, relative to housekeeping gene GAPDH and normalized to percentage of TH-positive cells in each sample as reported in Fig. 3B (*n* = 13, 11, 10, and 7, respectively). (**C**) Quantification of AADC protein relative to GAPDH (*n* = 3 per line). (**D**) Cropped immunoblot of total MAO-A, MAO-B, and GAPDH at day 65. (**E**) Quantification of MAO-A protein relative to GAPDH (*n* = 3 per line). (**F**) Quantification of relative MAO-B abundance in control and patient-derived neurons (*n* = 3 per line). (**G**) Immunofluorescence analysis of MAO-A/TH and MAO-A/GFAP (left) and MAO-B/TH and MAO-B/GFAP (right) in Control mDA neural culture at day 65 of differentiation. Nuclei were counterstained with DAPI (blue). Scale bar, 20 μm. (**H**) qRT-PCR for *MAO-A* at day 65 in Control: Patient 1, Patient 2, and CRISPR. mRNA values are relative to the mDA related gene *PITX3* and normalized to control (*n* =

3, 3, 3, and 5 respectively). Error bars indicate SEM. Both DTDS lines were independently compared to controls using two-tailed Student's *t* test for all analyses.

Europe PMC Funders Author Manuscripts

Europe PMC Funders Author Manuscripts

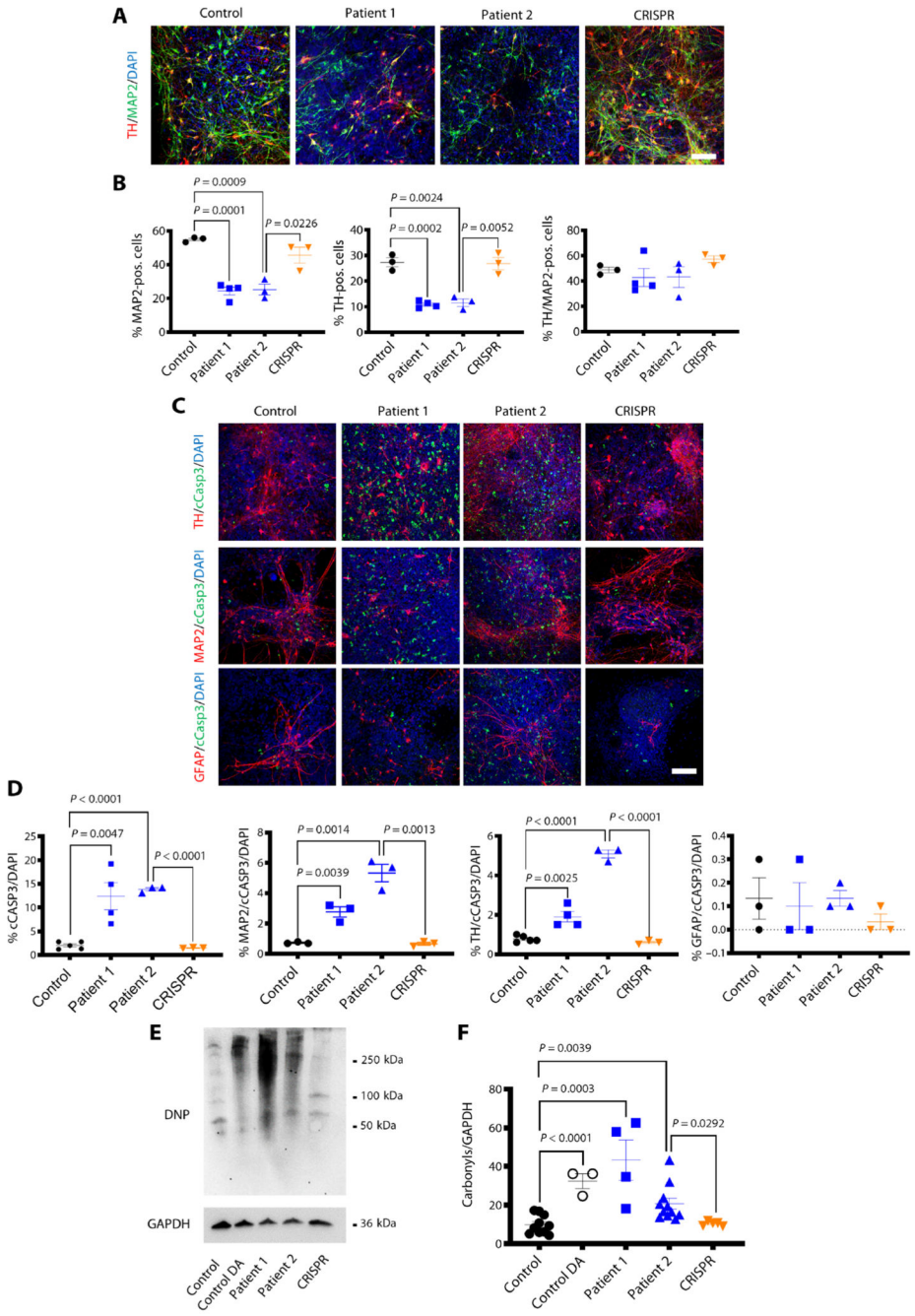

Fig. 3. DAT dysfunction in DTDS is associated with neurotoxicity and apoptotic neurodegeneration.

(**A**) Immunofluorescence analysis for neuronal markers TH/MAP2 at day 65. Nuclei were counterstained with DAPI. Scale bar, 100 μm. (**B**) Quantification of MAP2-positive, TH-positive, and TH/MAP2−double-positive neurons for control, patient 1, patient 2, and CRISPR-derived neuronal populations (n = 3, 4, 3, and 3, respectively). (**C**) Immunofluorescence analysis for TH/cCASP3, MAP2/cCASP3, and GFAP/cCASP3 at d65. Nuclei were stained for DAPI. Scale bar, 100 μm. (**D**) Quantification of total number of

cCASP3-positive cells, MAP2/cCASP3, TH/cCASP3, and GFAP/cCASP3−double-positive cells in control, patient 1, patient 2, and CRISPR-derived neuronal populations (n = 5, 4, 3, and 3, respectively; n = 3, 3, 3, and 3, respectively; n = 5, 4, 3, and 3, respectively; and n = 3, 3, 3, and 3, respectively). (**E**) Immunoblot of total carbonyls detected in mDA neurons at day 65 derived from control, control treated with 100 μM dopamine (DA), patient 1, patient 2, and CRISPR. (**F**) Quantification of total carbonyls relative to GAPDH (n = 10, 3, 4, 11, and 5, respectively). Error bars indicate SEM. Both DTDS lines were independently compared to controls using two-tailed Student's t test.

Europe PMC Funders Author Manuscripts

Europe PMC Funders Author Manuscripts

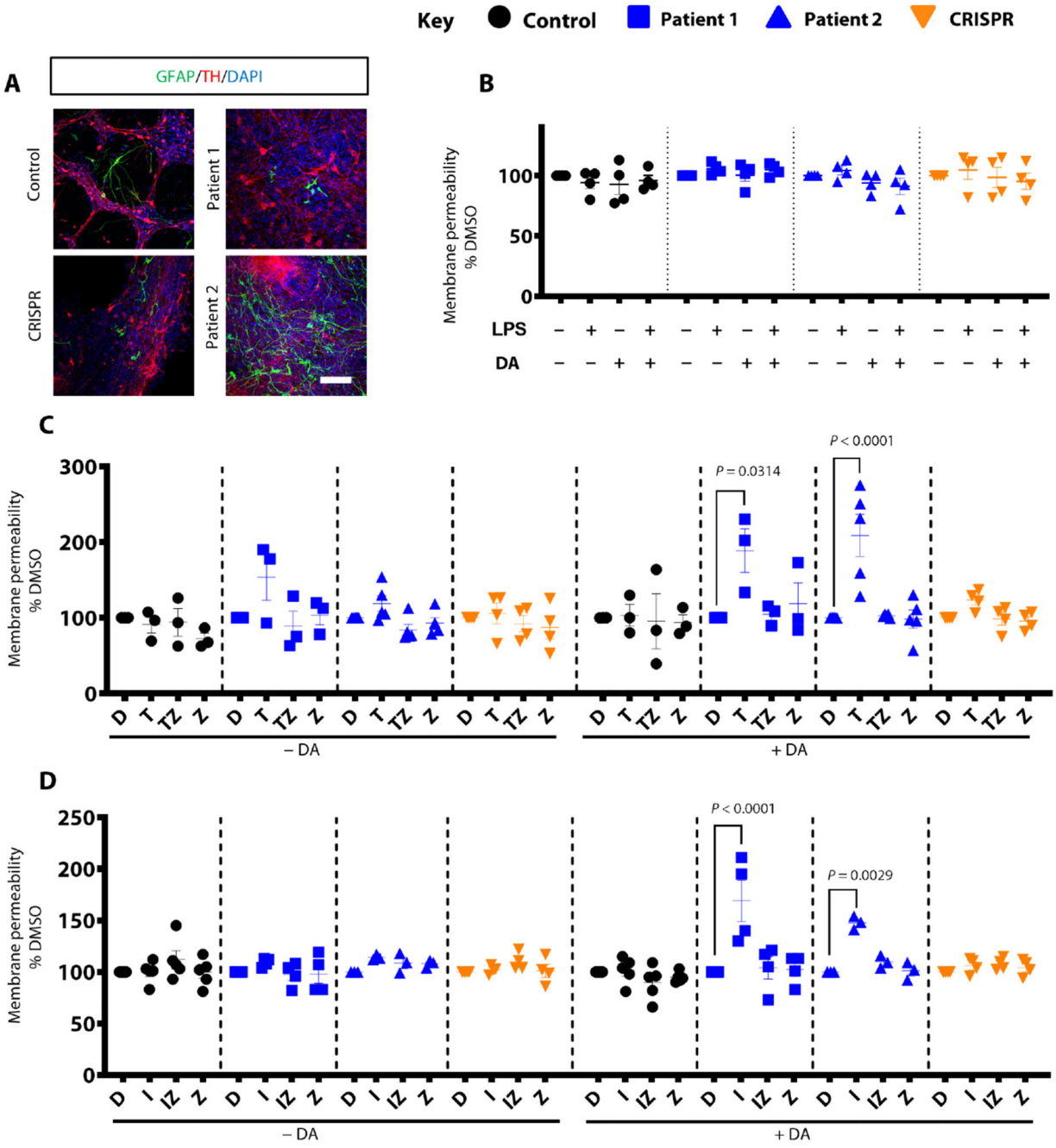

Fig. 4. Exposure of patient-derived mDA cultures to DA and proinflammatory cytokines induces neurodegeneration.

(**A**) Immunofluorescence analysis for GFAP and TH at day 65; nuclei are stained with DAPI. Scale bar, 100 μm. (**B**) Analysis of membrane permeability at day 65 for derived neuronal cultures treated with 100 μM DA and LPS (n = 4, 4, 4, and 4 for control, patient 1, patient 2, and CRISPR, respectively). Results are normalized to the dimethyl sulfoxide (DMSO) condition. (**C** and **D**) Membrane permeability at day 65 of differentiation. Cells were treated for 24 hours with DMSO (D), TNFα (T), or IL-1β (I), TNFα or IL-1β +

Z-VAD-FMK (TZ; IZ), or just Z-VAD-FMK (Z). DA was added at a concentration of 100 μM (n = 3, 3, 5, and 4 for each line; n = 5, 4, 3, and 4 respectively). Results are normalized to the DMSO-treated condition. Error bars indicate SEM. ANOVA was applied to allow multiple comparisons with normalized control.

Europe PMC Funders Author Manuscripts

Europe PMC Funders Author Manuscripts

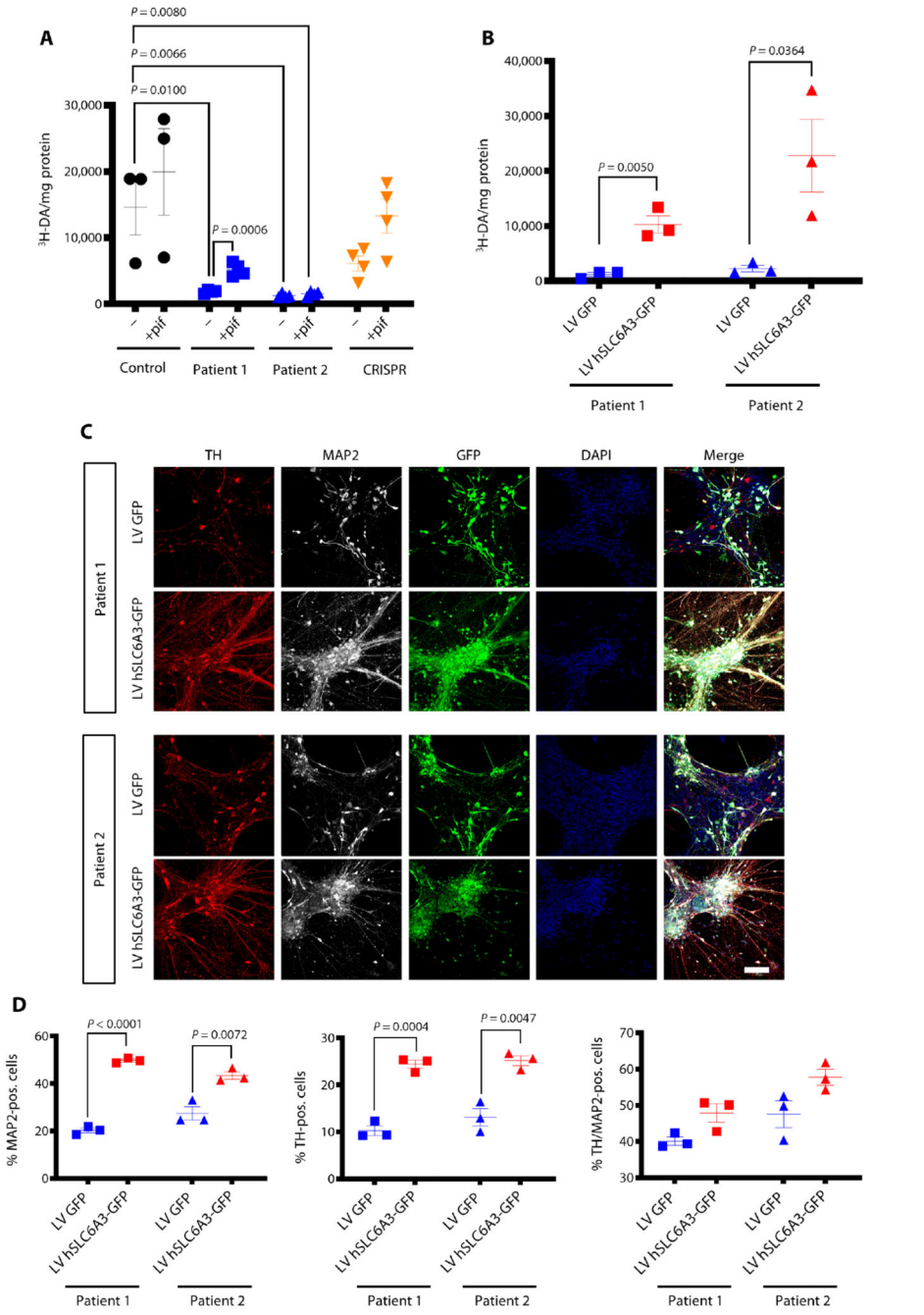

Fig. 5. Loss of DAT function in DTDS can be restored both pharmacologically and using a gene therapy approach in the mDA model.

(**A**) Uptake of tritiated DA at day 65 after neurons treated for 24 hour with pifithrin-μ (pif). Values are relative to protein concentration (n = 3, 4, 4, and 4 per line). (**B**) Measurement of tritiated DA uptake at day 65 in patient-derived mDA neurons transduced with either a lentivirus construct expressing GFP alone (LV GFP) or human *SLC6A3* and GFP (LV hSLC6A3-GFP) (n = 3 for each). (**C**) Immunofluorescence analysis at day 65 for patient-derived dopaminergic neurons transduced with LV GFP or LV hSLC6A3-GFP. Cells are

stained for TH/MAP2, and nuclei were counterstained with DAPI. Scale bar, 100 μm. (**D**) Quantification of MAP2-positive, TH-positive, and TH/MAP2− double-positive neurons at day 65 of differentiation in mDA neurons transduced with LV GFP or LV hSLC6A3-GFP (n = 3 for each). Both DTDS lines were independently compared to controls using two-tailed Student's t test for all analyses.

Europe PMC Funders Author Manuscripts

Europe PMC Funders Author Manuscripts

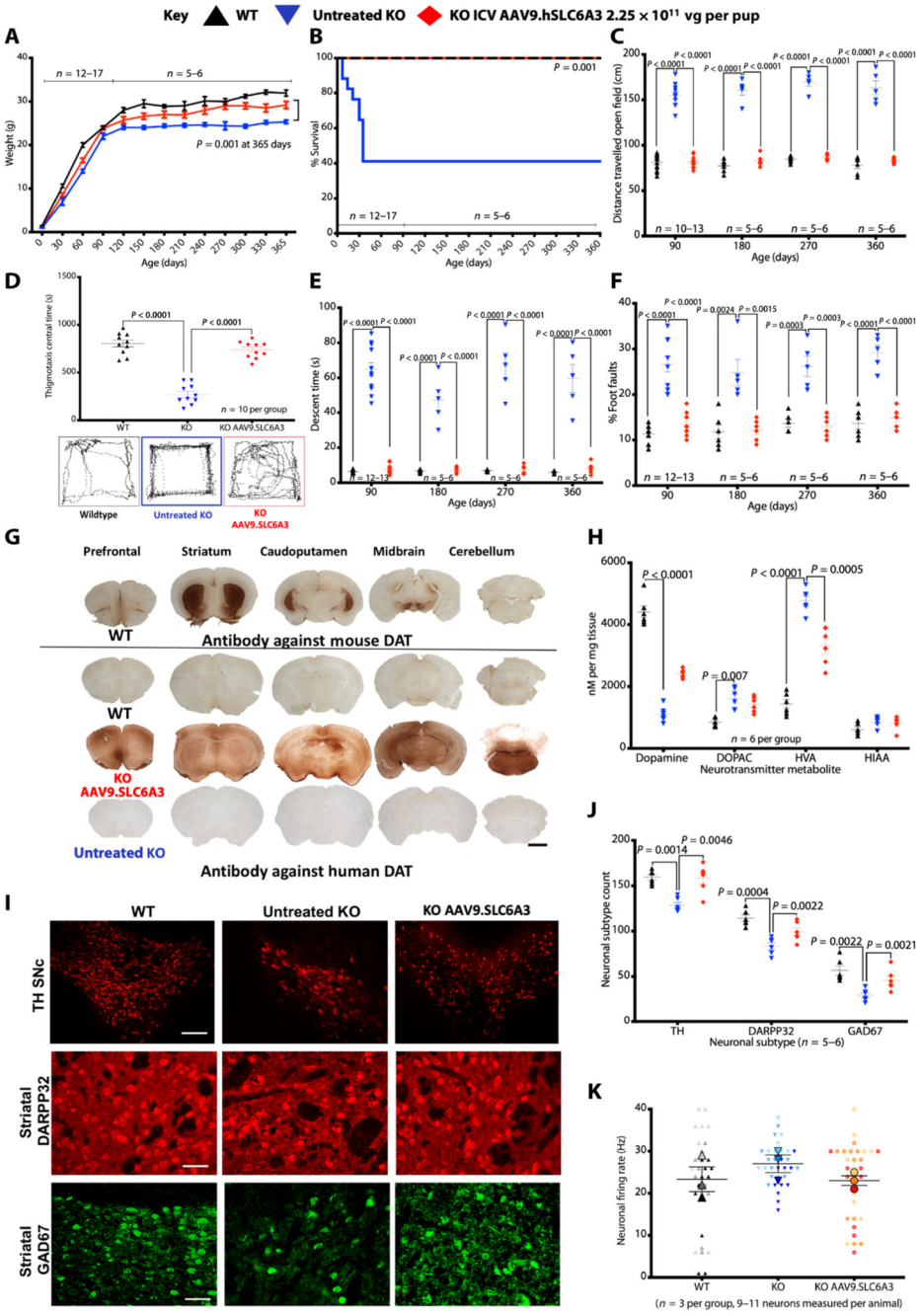

Fig. 6. Neonatal intracerebroventricular gene therapy to DAT knockouts.

(**A**) Weights of mice [2.25×10^{10} vg per pup; treated knockout (KO), $n = 13$; wild-type (WT), $n = 12$; untreated knockout, $n = 17$] (data are means ± SEM, Student's one-tailed t test on weight at 365 days untreated knockout versus treated). (**B**) Kaplan-Meier survival plot of wild-type, untreated knockout, and intracerebroventricular AAV9.SLC6A3 gene therapy− treated knockout (log-rank, Mantel-Cox test). (**C**) Locomotor assessment of mice in open field with distance traveled. (**D**) Central time and thigmotaxis with representative open field traces for each group. (**E**) Vertical pole descent time. (**F**) Foot faults (data

Europe PMC Funders Author Manuscripts

are means ± SEM; two-way ANOVA, log-transformed data for percentage of foot fault, and Bonferroni's multiple comparison test; group sizes as stated). (**G**) Representative immunostaining for mouse DAT in wild-type mice for physiological expression reference. Immuno-staining for hDAT in treated knockout, untreated knockout, and wild-type mice (scale bar, 1 mm; $n = 5$ per group). (**H**) DA and serotonin neurotransmitter metabolites from whole-brain homogenates analyzed by HPLC (data are means ± SEM; twoway ANOVA and Bonferroni's multiple comparison test; $n = 6$ per group). (**I**) Representative immunofluorescence for cell types TH mDA neurons (scale bar, 250 μm) and striatal DARPP32 and GAD67 neurons (scale bar, 100 μm) in wild-type, untreated knockout, and knockout hDAT treated mice ($n = 5$ to 6 per group). Data are means ± SEM. (**J**) Quantification of TH, DARP32, and GAD67 neurons in wild-type, untreated knockout, and knockout AAV9.SLC6A3 treated mice (data are means ± SEM; two-way ANOVA and Tukey's multiple comparison test; $n = 5$ per group). (**K**) Patch clamp electrophysiology of striatal medium spiny neurons ($n = 3$ animals per group with 9 to 11 neurons measured per animal). Data are means per animal ± SEM of group.

Europe PMC Funders Author Manuscripts

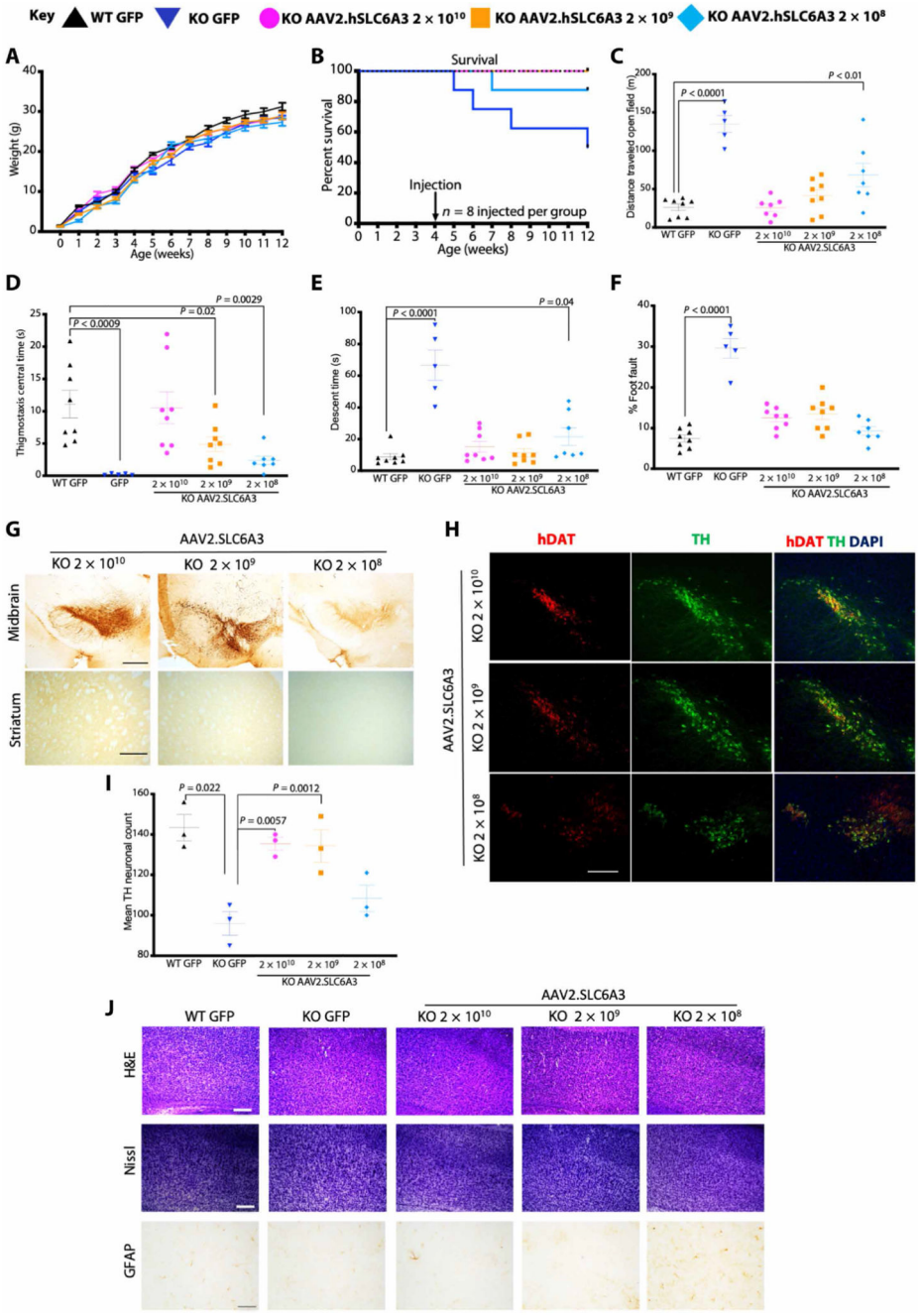

Fig. 7. Adult stereotactic AAV2 gene therapy to DAT knockout mice 2 log dose-ranging study.

(**A**) Weights of mice receiving stereotactic injected AAV2.SLC6A3 vector treated knockouts at three dosages: 2×10^{10}, 2×10^{9}, and 2×10^{8} vg per mouse. Control, wild-type, and knockout animals received AAV2.GFP vector, 2×10^{10} vg per mouse (data are means ± SEM; $n = 8$ per group). (**B**) Kaplan-Meier survival plot of WT AAV2.GFP, knockout AAV2.GFP, and treated knockout AAV2.SLC6A3 2×10^{10}, 2×10^{9}, and 2×10^{8} vg per mouse dosage groups. (**C**) Locomotor assessment of mice at 12 weeks (8 weeks after gene transfer) in open field with distance traveled. (**D**) Thigmotaxis central time. (**E**) Vertical pole

descent time. (**F**) Foot faults (data are means ±SEM; two-way ANOVA, log-transformed data for percentage of foot fault, and Bonferroni's multiple comparison test; $n = 5$ to 8 animals per group). (**G**) Representative immunostaining of midbrain and striatum for hDAT in AAV2.SLC6A3-treated knockout mice at 2×10^{10}, 2×10^{9}, and 2×10^{8} vg per mouse dosages (scale bars, 100 μm; $n = 3$ per group). (**H**) Representative doublel-abeled immunofluorescence for TH mDA neurons coexpressing hDAT in AAV2.SLC6A3-treated knockout mice at 2×10^{10}, 2×10^{9}, and 2×10^{8} vg per mouse (scale bar, 250 μm; $n = 3$ per group). (**I**) Quantification of TH neurons of AAV2.SLC6A3-treated knockouts at 2×10^{10}, 2×10^{9}, and 2×10^{8} vg per mouse (data means ± SEM; two-way ANOVA, $n = 3$ group). (**J**) Neurohistological panel showing frontal cortex of wild-type AAV2.GFP, knockout AAV2.GFP, and knockout AAV2.SLC6A3-treated mice at 2×10^{10}, 2×10^{9}, and 2×10^{8} vg per mouse. Representative images of hematoxylin and eosin (H&E) and Nissl stain (scale bar, 250 μm). Immunohistochemistry for GFAP in frontal cortex (scale bar, 100 μm; $n = 3$ per group for each panel).